

found for other dimetal complexes that contain dmpm bridges¹⁶ but upfield from the three sets of methylene resonances found in the spectrum of the triply bonded complex $\text{Re}_2(\mu\text{-dmpm})_3\text{Cl}_4$ (δ +4.71, +4.10, and +3.95).⁷ This difference may be due to a larger diamagnetic anisotropy in the triply bonded rhenium complex than in this quadruply bonded dimolybdenum compound.^{2,7}

The electronic absorption spectrum of a dichloromethane solution exhibits two absorptions in the region between 350 and 820 nm, at 426 nm ($\epsilon = 270$) and 604 nm ($\epsilon = 1730$). The feature at 604 nm is attributed to the $\delta^2 \rightarrow (\delta\delta^*)$ transition and represents a shift to higher energy compared to the band for $\text{Mo}_2(\mu\text{-dppm})_2\text{Cl}_4$ (634 nm).¹⁰ This energy shift correlates with an increase in the basicity of the phosphine ligand.

The electrochemical properties of **1** were examined in several solvents with use of the cyclic voltammetric technique. The compound is most soluble in dichloromethane, and solutions in this solvent, with 0.1 M TBAH as supporting electrolyte, exhibit a reversible process ($i_{p,a}/i_{p,c} \approx 1$) at +0.49 V vs. Ag/AgCl; this corresponds to a one-electron oxidation of the bulk complex. A second irreversible oxidation is observed with $E_{p,a} = +1.25$ V vs. Ag/AgCl, and an irreversible reduction can be seen near the solvent limit with $E_{p,c} = -1.75$ V vs. Ag/AgCl. These redox processes agree closely with those that characterize solutions of $\text{Mo}_2(\mu\text{-dppm})_2\text{Cl}_4$ in 0.1 M TBAH/ CH_2Cl_2 for which we see $E_{1/2}(\text{ox}) = +0.66$ V and $E_{p,c} = -1.50$ V vs. Ag/AgCl.¹⁰ Although the oxidation at +0.49 V approaches electrochemical reversibility in this solvent system ($\Delta E_p = 110$ mV at $v = 200$ mV/s), the cation formed is unstable chemically. Bulk electrolysis of 0.1 M TBAH/ CH_2Cl_2 solutions of **1** at +0.70 V resulted in a rapid decomposition of the cation.

When either acetonitrile or THF is used as the solvent in these electrochemical measurements, the reversible oxidation observed in CH_2Cl_2 now becomes irreversible and the potentials at which the electrochemical processes occur are shifted. In 0.1 M

TBAH/ CH_3CN , one irreversible oxidation is observed at $E_{p,a} = +0.31$ V vs. Ag/AgCl and an irreversible reduction at $E_{p,c} = -1.52$ V vs. Ag/AgCl. In 0.2 M TBAH/THF solutions these processes shift to more positive potentials at $E_{p,a} = +0.45$ V and $E_{1/2} = -1.50$ V vs. a silver quasi reference electrode. Note that the process at -1.50 V looks reasonably reversible provided a switching potential of ca. -1.75 V is used. However, when the measurements are extended to ca. -2.5 V, product waves are seen at $E_{p,c} = -1.90$ and -2.20 V and the $i_{p,c}/i_{p,a}$ ratio for a couple at -1.50 V is now much greater than unity.^{18,19}

Acknowledgment. Support from the National Science Foundation (Grant No. CHE 85-06702 to R.A.W. and Grant No. CHE-8514588 to F.A.C.) is gratefully acknowledged. We also thank Professor I. P. Rowell for making the results cited in ref 17 available to us.

Registry No. $\text{Mo}_2(\mu\text{-dmpm})_2\text{Cl}_4 \cdot 1/2\text{H}_2\text{O} \cdot 5/4\text{CH}_3\text{OH}$, 104092-00-4; $\text{Mo}_2(\text{O}_2\text{CCH}_3)_4$, 14221-06-8; $\text{K}_4\text{Mo}_2\text{Cl}_8$, 25448-39-9; Mo, 7439-98-7.

Supplementary Material Available: Tables of anisotropic displacement parameters for both structures and a table of torsion angles for the monoclinic structure (3 pages); tables of observed and calculated structure factors for both structures (14 pages). Ordering information is given on any current masthead page.

- (18) Under our experimental conditions the ferrocenium/ferrocene couple has $E_{1/2} = 0.47$ V vs. the Ag/AgCl and silver quasi reference electrodes in 0.1 M TBAH/ CH_2Cl_2 and 0.2 M TBAH/THF, respectively.
- (19) We note that the cyclic voltammogram of $\text{Mo}_2(\mu\text{-dmpm})_2\text{Cl}_4$ in THF is quite different from that of $\text{Mo}_2(\mu\text{-dmpm})_2(\text{OAr})_4$ (OAr = 3,5-dimethylphenoxide).¹⁷ This aryloxide complex exhibits two reversible processes corresponding to oxidations at $E_{1/2} = +0.10$ and -0.40 V vs. a silver quasi reference electrode. Two reductions are also observed, the first with $E_{1/2} = -1.40$ V and the second with $E_{p,c} = -2.00$ V vs. the silver quasi reference electrode. This apparently reflects the strong π -donor capability of alkoxide ligands and the consequent electron-rich nature of the metal centers.

Contribution from the Departments of Chemistry, University of Wisconsin—Milwaukee, Milwaukee, Wisconsin 53201, and Northeastern University, Boston, Massachusetts 02115

Solid-State Structure and Solution Equilibria of Cyano(triethylphosphine)gold(I)

Anne L. Hormann,[†] C. Frank Shaw III,^{*†} Dennis W. Bennett,[†] and W. M. Reiff[†]

Received January 30, 1986

The solid-state structure and solution equilibria of cyano(triethylphosphine)gold have been investigated. Et_3PAuCN crystallizes in the orthorhombic lattice $Pbca$ with $a = 6.6711$ (7) Å, $b = 15.002$ (1) Å, $c = 19.439$ (2) Å, and $Z = 8$. The Au-P distance is 228.8 (5) pm, and the Au-C distance is 197 (2) pm. $\angle\text{CAuP} = 176.6$ (6)°. The structure was refined to $R = 0.061$. The ¹⁹⁷Au Mössbauer parameters are $\text{IS} = 4.69$ mm/s and $\text{QS} = 9.56$ mm/s, consistent with a linear, two-coordinate structure. IR and ¹³C{¹H} and ³¹P{¹H} NMR studies show that in solution Et_3PAuCN disproportionates to form $\text{Au}(\text{CN})_2^-$ and $(\text{Et}_3\text{P})_2\text{Au}^+$. The equilibrium constant for the disproportionation of Et_3PAuCN is solvent-dependent: $K_{\text{eq}} = 0.06$ (CDCl_3), 0.13 (C_6D_6), and 0.88 (CH_3OD). The solution chemistry of Ph_3PAuCN was also studied by ³¹P and ¹³C NMR. At 297 K Ph_3PAuCN is in rapid equilibrium with $(\text{Ph}_3\text{P})_2\text{Au}^+$ and $\text{Au}(\text{CN})_2^-$, but at 200 K resonances for all three species are observed. These results suggest that, in some cases, the disproportionation of LAuX complexes may be masked by rapid ligand exchange.

Introduction

Gold(I) has a strong but not exclusive tendency to form linear two-coordinate complexes, LAuX , where L is a neutral Lewis base (e.g. phosphine, thioether, etc.) and X is an aryl or alkyl group, halide, or pseudohalide.¹⁻³ These complexes are usually formulated as neutral complexes, LAuX , but since gold(I) is generally labile, there exists the possibility of ligand scrambling to form the symmetrically substituted complexes AuL_2^+ and AuX_2^- . Indeed, (tetrahydrothiophene)gold iodide in the solid state contains the ions $[\text{Au}(\text{THF})_2^+][\text{AuI}_2^-]$ linked by weak gold-gold interactions,⁴ and anionic cyano(thiolato)gold(I) complexes, RSAuCN^- , in

aqueous solution are in equilibrium with substantial concentrations of $\text{Au}(\text{CN})_2^-$ and $\text{Au}(\text{SR})_2^-$.⁵ Similar ligand-scrambling reactions may significantly alter the solution chemistry of gold(I) complexes such as the new antiarthritic drug auranofin, which is a (phosphine)gold(I) thiolate. Since ³¹P and ¹³C NMR can probe each ligand directly, R_3PAuCN complexes are useful model systems for examining the ligand-scrambling reactions of gold(I) complexes. Therefore, we have undertaken a detailed study of the

- (1) Bellon, P. L.; Manassero, M.; Sansoni, M. *Ric. Sci.* **1969**, *39*, 173.
 (2) Gavens, P. D.; Guy, J. J.; Mays, M. J.; Sheldrick, G. M. *Acta Crystallogr., Sect. B: Struct. Crystallogr. Cryst. Chem.* **1977**, *B33*, 137.
 (3) Baenziger, N. C.; Bennett, W. E.; Soboroff, D. M. *Acta Crystallogr., Sect. B: Struct. Crystallogr. Cryst. Chem.* **1976**, *B32*, 962.
 (4) Ahrland, S.; Noren, B.; Oskarsson, A. *Inorg. Chem.* **1985**, *24*, 1330.
 (5) Shaw, C. F., III; Lewis, G. *Inorg. Chem.* **1986**, *25*, 58.

[†]University of Wisconsin—Milwaukee.

[†]Northeastern University.

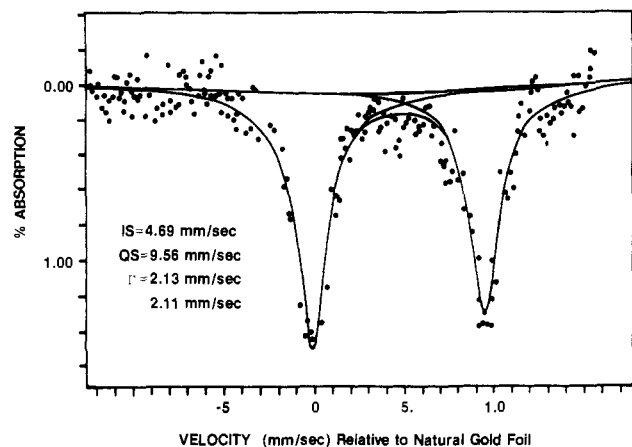


Figure 1. Mössbauer spectrum of Et_3PAuCN at 4.2 K. IS is reported vs. gold foil.

solid-state structure of Et_3PAuCN and solution chemistry of Et_3PAuCN and Ph_3PAuCN .

Experimental Section

Reagents. Deuterated chloroform and methanol- d_1 were obtained from Aldrich, and benzene- d_6 was purchased from Sigma. 99% K^{13}CN and deuterated dimethyl sulfoxide were purchased from Stohler Isotope Chemicals. Chloro(triethylphosphine)gold(I) was provided by Smith Kline and French Laboratories. Ph_3PAuCl was prepared by the method of McAuliffe et al.⁶ using HAuCl_4 . All other reagents were of ACS quality.

Preparation of Cyano(triethylphosphine)gold(I).⁷ To a solution of 0.4858 g (1.39 mmol) of chloro(triethylphosphine)gold in 35 mL of toluene was added a solution of 0.1060 g (1.63 mmol) of potassium cyanide in 10 mL of double-distilled water. (For $\text{Et}_3\text{PAu}^{13}\text{CN}$ 30% of the potassium cyanide used was K^{13}CN). After the mixture was stirred for 3–4 h, the toluene layer was isolated, dried over sodium sulfate, and concentrated. Addition of diethyl ether and chilling resulted in the precipitation of fine white crystals, which were filtered and washed with cold diethyl ether to give 0.3334 g (0.98 mmol, 70.5%) of Et_3PAuCN : mp 112.7–113.1 °C; $\nu_{\text{CN}} = 2138 \text{ cm}^{-1}$. Anal. Calcd for $\text{C}_7\text{H}_{15}\text{AuNP}$: C, 24.65; H, 4.43; N, 4.11. Found: C, 24.73; H, 4.40; N, 4.06.

Preparation of Cyano(triphenylphosphine)gold(I). To a solution of 0.6705 g (1.36 mmol) of chloro(triphenylphosphine)gold in 55 mL of acetone was added a solution of 0.0686 g (1.05 mmol) of KCN and 0.0250 g (0.378 mmol) of K^{13}CN in 15 mL of double-distilled water. After the mixture was stirred for 1/2 h, the solvent was removed in vacuo, leaving a white precipitate. It was washed three times with water and then with diethyl ether. Obtained was 0.3117 g (47.4%) of a white solid: mp 201 °C (lit. mp 204 °C⁸); $\nu_{\text{CN}} = 2147 \text{ cm}^{-1}$ (lit. $\nu_{\text{CN}} 2146 \text{ cm}^{-1}$ ⁹). Anal. Calcd for $\text{C}_{19}\text{H}_{15}\text{AuNP}$: C, 47.02; H, 3.12; N, 2.89. Found: C, 47.24; H, 3.13; N, 2.93.

Vibrational Spectra. Infrared (IR) spectra of the complexes from 4800 to 400 cm^{-1} were recorded on a Nicolet MX1 spectrophotometer as Nujol mulls on KBr plates or as chloroform, benzene, methanol, or dimethyl sulfoxide solutions in KBr cells with a 0.1-mm path length.

$^{31}\text{P}\{^1\text{H}\}$ and $^{13}\text{C}\{^1\text{H}\}$ Nuclear Magnetic Resonance Spectra. $^{31}\text{P}\{^1\text{H}\}$ and $^{13}\text{C}\{^1\text{H}\}$ spectra (at 297 K) were obtained in CDCl_3 , C_6D_6 , CH_3OD , and $(\text{CD}_3)_2\text{SO}$ on a Bruker WP 250 multinuclear spectrometer at 101.3 and 62.9 MHz, respectively. Concentrations for both the ^{31}P and ^{13}C NMR samples ranged from ~0.05 to 0.1 M. Chemical shifts were measured relative to trimethyl phosphate and tetramethylsilane for the ^{31}P and ^{13}C spectra, respectively. For the ^{13}C spectra Et_3PAuCN and Ph_3PAuCN were enriched with ^{13}C to shorten the acquisition time, since metal-bound cyanide species have long T_1 's.¹⁰ The ^{13}C -enriched complexes were also used to verify peak assignments, via $^2J_{\text{PC}}$ coupling, in the ^{31}P spectra. T_1 values were determined for the two phosphine species present in the Et_3PAuCN solutions by the inversion recovery method. The ^{31}P NMR spectra were then accumulated under appropriate conditions (e.g.,

Table I. Summary of Crystal Data and X-ray Intensity Collection for Et_3PAuCN

cryst syst	orthorhombic
space group	<i>Pbca</i> (No. 61)
cryst dimens, mm	0.30 × 0.27 × 0.21
cell params (25 °C)	
<i>a</i> , Å	6.6711 (7)
<i>b</i> , Å	15.0022 (12)
<i>c</i> , Å	19.4393 (21)
<i>V</i> , Å ³	1945.51
<i>Z</i>	8
calcd density, g/cm ³	2.33
abs coeff, cm ⁻¹	157.18
formula	$\text{C}_7\text{H}_{15}\text{AuNP}$
fw	341.2
diffractometer	Picker/Krisel
radiation (λ , Å)	$\text{Mo K}\alpha$ (0.710 69), Zr filtered
scan type; range, deg	θ - 2θ ; $2\theta = 4$ –55
scan rate	variable (constant precision scans)
no. of obsd reflns	1323 ($I_o > 2.5\sigma(I_o)$)
refinement	full-matrix least squares
R^a	0.061
R_w^b	0.066

$$^a R = [\sum(|F_o| - |F_c|)] / (\sum|F_o|). \quad ^b R_w = (\sum[w^{1/2}(|F_o| - |F_c|)]) / \sum(w^{1/2}|F_o|); w = 1.4580 / (\sigma^2(F) + 0.002011 F^2).$$

Table II. Positional Parameters and Esd's for Et_3PAuCN

atom	<i>x/a</i>	<i>y/b</i>	<i>z/c</i>
Au	0.2728 (1)	0.5315 (0)	0.2593 (0)
P	0.2360 (7)	0.3842 (3)	0.8573 (2)
C(7)	0.227 (3)	0.547 (1)	0.678 (1)
N	0.288 (3)	0.589 (2)	0.629 (1)
C(1)	-0.012 (3)	0.345 (1)	0.884 (1)
C(2)	-0.012 (3)	0.287 (2)	0.948 (1)
C(3)	0.396 (3)	0.286 (1)	0.852 (1)
C(4)	0.331 (3)	0.220 (1)	0.797 (1)
C(5)	0.338 (3)	0.444 (2)	0.932 (1)
C(6)	0.232 (4)	0.534 (2)	0.942 (1)

pulse angle 45° and delay time 50 s for $T_1 = 10$ –12 s) so that they could be quantitatively integrated.

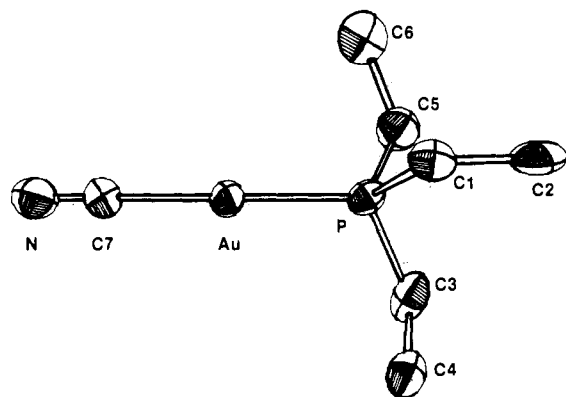
Mössbauer Spectrum. The ^{197}Au Mössbauer spectrum (Figure 1) was obtained on 100 mg of powdered crystals that were contained in a Nylon holder of 12-mm diameter. The holder was wrapped in aluminum foil and maintained at 4.2 K throughout the data collection. The instrumentation used was previously described,¹¹ and the integrating counting technique was used.¹² The recorded spectrum was fitted to a pair of Lorentzian lines, and the isomer shift was measured with respect to gold foil.

X-ray Data Collection. A summary of crystal and intensity collection data is presented in Table I. A single colorless crystal of Et_3PAuCN was obtained by slow diffusion of diethyl ether into a chloroform solution of Et_3PAuCN . The crystal was mounted in a 0.5-mm capillary that was sealed with epoxy. The unit cell dimensions were determined by a least-squares refinement of 15 accurately centered reflections. The intensities of 3 standard reflections that were checked every 2 h showed an approximate 19% intensity loss during data collection, thus limiting the amount of data collected. Empirical absorption corrections were made by collecting ψ -scan intensity and interpolating transmission factors using the program Camel Jockey.¹³

Solution and Refinement of the Structure. The structure was solved and refined by using SHELX.¹⁴ The gold atom was located by direct methods with the remaining non-hydrogen atoms located by standard difference Fourier techniques. The positions of the hydrogen atoms were calculated from ideal methyl and methylene geometries. Each hydrogen atom was assigned an isotropic temperature factor 1.2 times the isotropic temperature factor of the carbon atom to which it was attached. The methyl groups were refined as rigid bodies with fixed C–H bond lengths of 108 pm and fixed H–C–H bond angles of 109.5°.

- McAuliffe, C. A.; Parish, R. V.; Randall, P. D. *J. Chem. Soc., Dalton Trans.* **1979**, 1730.
- Personal communication from D. T. Hill of Smith Kline and French Laboratories.
- Burmeister, J. L.; Melpolder, J. B. *Inorg. Chim. Acta* **1981**, *49*, 115.
- Cariati, F.; Galizzoli, D.; Naldini, L. *Chim. Ind. (Milan)* **1970**, *52*, 995.
- Pesek, J. J.; Mason, R. W. *Inorg. Chem.* **1979**, *18*, 924.

- Viegers, M. P. A. Thesis, University of Nijmegen, The Netherlands, 1974.
- Viegers, M. P. A.; Trooster, J. M. *Nucl. Instrum. Methods* **1976**, *118*, 257.
- Flack, H. D. *J. Appl. Crystallogr.* **1975**, *8*, 520 (Part 5).
- Sheldrick, G. M. "SHELX-76, A Program for Crystal Structure Determination"; University of Cambridge: Cambridge, England, 1976.

Figure 2. Structure of Et₃PAuCN.Table III. Selected Bond Distances and Angles for Et₃PAuCN

Interatomic Distances (pm)			
Au-P	228.8 (5)	P-C(5)	183 (2)
Au-C(7)	197 (2)	C(1)-C(2)	151 (3)
C(7)-N	115 (3)	C(3)-C(4)	152 (3)
P-C(1)	183 (2)	C(5)-C(6)	153 (3)
P-C(3)	182 (2)		
Interatomic Angles (deg)			
N-C(7)-Au	177 (2)	Au-P-C(5)	113.2 (7)
C(7)-Au-P	176.6 (6)	P-C(1)-C(2)	115 (1)
Au-P-C(1)	113.0 (7)	P-C(3)-C(4)	114 (2)
Au-P-C(3)	114.6 (8)	P-C(5)-C(6)	111 (2)

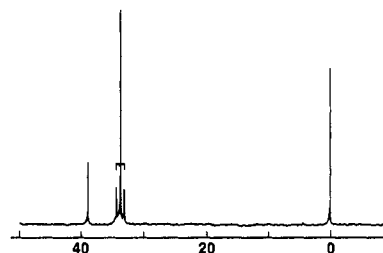
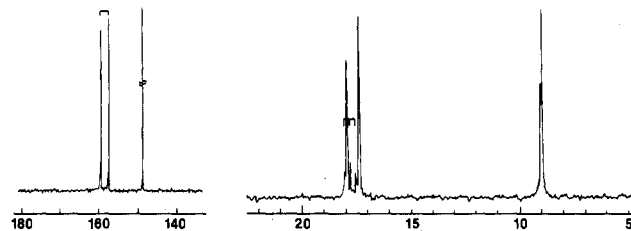
Initial heavy-atom refinement ($R = 0.075$) revealed two large ghost peaks (ca. $3.1 \text{ e}/\text{\AA}^3$ and $2.8 \text{ e}/\text{\AA}^3$) located within 0.8 \AA of the gold and phosphorus atoms, respectively, in the asymmetric unit. An analysis of the F_o/F_c list indicated that nearly all reflections with significant differences in F_o and F_c had $|F_o| < |F_c|$, indicating substantial secondary extinction. Fourteen of the reflections had F_o/F_c ratios less than 0.75 and were omitted from the final refinement. After removal of these reflections, changes in atomic or thermal parameters were negligible (~ 1 esd) with R decreasing to 0.061 and the ghost peaks shifting slightly, decreasing in intensity ($2.6 \text{ e}/\text{\AA}^3$ and $2.1 \text{ e}/\text{\AA}^3$) but still remaining within chemically unreasonable distances of the gold and phosphorus atoms. The final positional parameters appear in Table II and in the supplementary material. Tables of observed and calculated structure factors and final thermal parameters are also included as supplementary material. An ORTEP drawing of Et₃PAuCN appears in Figure 2, and the corresponding bond distances and angles are in Table III.

Results

The IR spectrum of solid Et₃PAuCN has one cyanide stretch at $\nu_{\text{CN}} = 2138 \text{ cm}^{-1}$. However, in both chloroform and benzene solutions there are two cyanide bands, $\nu_{\text{CN}} = 2143$ and 2149 cm^{-1} and $\nu_{\text{CN}} = 2141$ and 2149 cm^{-1} , respectively. The appearance of a second cyanide band for Et₃PAuCN in solution can be explained by the equilibrium



To characterize Et₃PAuCN in the solid state and to ascertain that the second cyanide band in the IR spectra was not due to an impurity, other techniques were employed. The Mössbauer spectrum of Et₃PAuCN (Figure 1) indicates that there is a single Au environment, $IS = 4.69 \text{ mm/s}$ (with respect to Au foil) and $QS = 9.56 \text{ mm/s}$. The crystal structure was also determined (Tables I and II and Figure 2), and it confirmed the existence of neutral Et₃PAuCN in the solid state. The principal bond lengths

Figure 3. ³¹P{¹H} NMR spectrum of Et₃PAu¹³CN (30% enriched) in CDCl₃ (0.05 M, $^2J_{\text{PC}} = 122.6 \text{ Hz}$).Figure 4. ¹³C{¹H} NMR spectrum of Et₃PAu¹³CN (30% enriched) in CDCl₃ (0.10 M, $^1J_{\text{PC}} = 35.1 \text{ Hz}$, $^2J_{\text{PC}} = 122.4 \text{ Hz}$, $^1J_{\text{PC}} + ^3J_{\text{PC}} = 16.3 \text{ Hz}$).

are $d(\text{AuP}) = 228.8 (5) \text{ pm}$ and $d(\text{AuC}) = 197 (2) \text{ pm}$, and bond angles are $\angle \text{NCAu} = 177 (2)^\circ$ and $\angle \text{CAuP} = 176.6 (6)^\circ$. Other selected bond distances and angles are in Table III. On the basis of these results and the excellent analytical data for the complex, we concluded that the second cyanide band arises from equilibrium 1.

The solution equilibrium of Et₃PAuCN was studied by IR spectroscopy. A second distinct cyanide band appears in the IR spectra of chloroform ($\nu_{\text{CN}} = 2143, 2149 \text{ cm}^{-1}$) and benzene ($\nu_{\text{CN}} = 2141, 2149 \text{ cm}^{-1}$) solutions and can be attributed to the ν_{as} of $\text{Au}(\text{CN})_2^-$ (eq 1). In methanol there is a principal cyanide band at 2151 cm^{-1} and a shoulder at 2160 cm^{-1} ; the envelope is slightly shifted and broader than that of $\text{KAu}(\text{CN})_2$ in methanol (2149 cm^{-1}). In dimethyl sulfoxide there is only one band at 2141 cm^{-1} , which is the same frequency as that observed for $\text{KAu}(\text{CN})_2$ in dimethyl sulfoxide, but again the band is broader, suggesting that there may be another band present.

³¹P NMR spectra further supported the proposed dissociation of Et₃PAuCN in solution. The two phosphorus resonances present (Figure 3, Table IV) can be explained by equilibrium 1 and assigned to Et₃PAuCN and the bis(phosphine) species $(\text{Et}_3\text{P})_2\text{Au}^+$. The assignment of the peaks was confirmed by preparing Et₃PAuCN enriched with 30% ¹³C and observing the doublet due to $^2J_{\text{PC}}$, which appears as satellites of the Et₃PAuCN resonances. In chloroform the peak at 33.6 ppm ($^2J_{\text{PC}} = 122.6 \text{ Hz}$) is assigned to Et₃PAu¹³CN (Figure 3). The peak at 38.8 ppm is due to $(\text{Et}_3\text{P})_2\text{Au}^+$. The resonances were also well resolved in methanol, but when dimethyl sulfoxide and benzene were used, the splitting due to Et₃PAu¹³CN was not completely resolved although the assignment of the peaks was still obvious and similar to those made in chloroform and methanol (Table IV). Thus, the peaks at 32–36 ppm in the various solvents were unambiguously assigned to Et₃PAu¹³CN while the peak that was further downfield and not split by ¹³C was assigned to $(\text{Et}_3\text{P})_2\text{Au}^+$.

To further characterize the equilibrium between the Et₃PAuCN, $\text{Au}(\text{CN})_2^-$, and $(\text{Et}_3\text{P})_2\text{Au}^+$ species, ¹³C spectra were obtained with 30%-enriched Et₃PAu¹³CN to shorten the acquisition time

Table IV. ³¹P{¹H} NMR Data for Et₃PAu¹³CN in Solution

solvent	Et ₃ PAu ¹³ CN			$(\text{Et}_3\text{P})_2\text{Au}^+$			e^b	u^c	K_{eq}
	δ^a	$^2J_{\text{PC}}$, Hz	T_1 , s	δ^a	T_1 , s				
CDCl ₃	33.6	122.6	9.83	38.8	11.60		4.8	1.9	0.06 (2)
C ₆ D ₆	32.1		8.64	37.9	8.45		2.3	0	0.13 (3)
CH ₃ OD	35.1	122.2	10.27	48.2	11.68		33	1.7	0.88 (6)
(CD ₃) ₂ SO	35.2		6.52	45.2	7.57		47	3.9	0.36 (3)

^aChemical shifts are given relative to trimethyl phosphate. ^bDielectric constant at 20 °C. ^cDipole moment in gas phase.

Table V. $^{13}\text{C}\{^1\text{H}\}$ NMR Data for $\text{Et}_3\text{PAu}^{13}\text{CN}$ in Solution^a

solvent	$\text{Et}_3\text{PAu}^{13}\text{CN}$					$\text{Au}(\text{CN})_2^-$	$(\text{Et}_3\text{P})_2\text{Au}^+$		
	δ_{CH_3}	δ_{CH_2}	$^1J_{\text{PC}}$, Hz	δ_{CN}	$^2J_{\text{PC}}$, Hz		δ_{CH_3}	δ_{CH_2}	J , Hz ^b
CDCl_3	8.97	17.7	35.1	158.2	122.4	148.6	9.02	17.8	16.3
C_6D_6	8.69	17.1	34.1	157.7	122.7	147.9	9.02	17.7 ^c	16.5
CH_3OD	9.38	18.2	35.1	160.4	122.2	151.4	9.46	18.4	17.0
$(\text{CD}_3)_2\text{SO}$	8.82	16.5		158.2		149.3			

^aChemical shifts are given relative to tetramethylsilane. ^b $J = ^1J_{\text{PC}} + ^3J_{\text{PC}}$. ^cThe third peak from virtual coupling is hidden underneath the peak assigned to the methylene carbon of $\text{Et}_3\text{PAu}^{13}\text{CN}$. The chemical shift given is that of the central peak, and the coupling constant is the frequency difference between the two peaks observed.

required to see the metal-bound cyanide species.¹⁰ The chemical shifts and coupling constants are summarized in Table V. For Et_3PAuCN in CDCl_3 (Figure 4), the following assignments were made. The singlet at 8.97 ppm was assigned to the methyl carbon, the doublet at 17.7 ppm ($^1J_{\text{PC}} = 35$ Hz) is the methylene carbon resonance that is split by the phosphorus, and the doublet that appears at 158.1 ppm arises from the ^{13}C that is split by the phosphorus. The coupling constant of 122.4 Hz is identical with the $^2J_{\text{PC}}$ value observed in the ^{31}P spectrum of $\text{Et}_3\text{PAu}^{13}\text{CN}$ (Table IV). The $\text{Au}(\text{CN})_2^-$ species gives a singlet that appears downfield at 148.6 ppm. The methyl carbons of the linear $(\text{Et}_3\text{P})_2\text{Au}^+$ ion give a singlet (9.02 ppm) that is almost coincident with the methyl carbon resonance of the Et_3PAuCN complex. The methylene carbons of $(\text{Et}_3\text{P})_2\text{Au}^+$ give rise to a triplet (17.8 ppm) that is close to the chemical shift of the methylene carbon in Et_3PAuCN . The triplet results from virtual coupling ($^1J_{\text{PC}} + ^3J_{\text{PC}} = 16.3$ Hz) of the two phosphorus nuclei. A similar triplet appears in the ^{13}C spectrum of *trans*- $\text{PdCl}_2(\text{P}-n\text{-Bu}_2\text{-}t\text{-Bu})_2$.¹⁵

Assignments of the ^{13}C spectra obtained in methanol and benzene are similar (Table V) and will not be discussed in detail. In dimethyl sulfoxide, the signals due to the methyl and methylene carbons of $(\text{Et}_3\text{P})_2\text{Au}^+$ were unresolved from those of Et_3PAuCN . Also, the peaks due to the methyl and methylene carbons of the Et_3PAuCN species were broader, and there was no observed $^1J_{\text{PC}}$ for the methylene carbon. The $\text{Au}(\text{CN})_2^-$ signal, however, remained as narrow ($\Delta\nu_{1/2} \sim 8$ Hz) as it was in the spectra obtained in the other solvents, suggesting that the peak broadening in Me_2SO is not a result of slower cyanide/triethylphosphine exchange in this solvent. Rather, it may be a result of ligand exchange between dimethyl sulfoxide and triethylphosphine or of Me_2SO coordination to form a three-coordinate gold(I) complex.

The equilibrium constants for the disproportionation of Et_3PAuCN in solution (eq 1) were determined by integrating the ^{31}P NMR spectra. First, the T_1 values of the Et_3PAuCN and $(\text{Et}_3\text{P})_2\text{Au}^+$ resonances were measured in each solvent by using the inversion recovery method (Table IV). These values, ranging from 8.5 to 11.5 s, are typical of other metal-phosphine complexes such as *trans*- $\text{PdCl}_2(\text{PEt}_3)_2$, where $T_1 = 9.5$ s in CDCl_3 at 30 °C.¹⁶ From the T_1 values, conditions for integration of the spectra were selected. The calculated K_{eq} values (Table IV) ranged from 0.06 to 0.88. One expects an increase in the value of K_{eq} with increased solvent polarity because the disproportionation produces charged species. The equilibrium constants for the two least polar solvents, CDCl_3 and C_6D_6 , were smaller, $K_{\text{eq}} = 0.06$ and 0.13, respectively, and that for CH_3OD is 0.88. The anomalously small value of $K_{\text{eq}} = 0.36$ in $(\text{CD}_3)_2\text{SO}$ may be due to exchange processes involving the solvent, as discussed above.

To determine whether the disproportionation reaction occurs for other cyanogold(I) complexes, the ^{31}P and ^{13}C spectra of the analogous complex, $\text{Ph}_3\text{PAu}^{13}\text{CN}$, were recorded in CH_3OD . At 297 K the ^{31}P spectrum (Figure 5) has only a single broad peak at 38.1 ppm. When the temperature was lowered to 200 K, peaks at 41.6 and 36.0 ppm were resolved and assigned, on the basis of the observed coupling constant, $^2J_{\text{PC}}$, to $(\text{Ph}_3\text{P})_2\text{Au}^+$ and $\text{Ph}_3\text{PAu}^{13}\text{CN}$, respectively. The latter species has a coupling

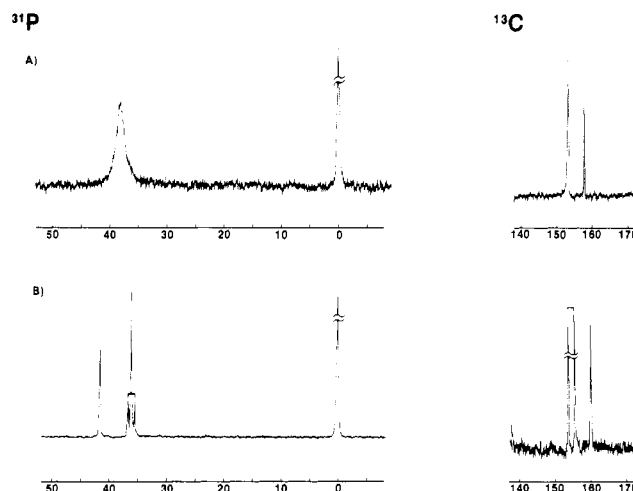


Figure 5. $^{31}\text{P}\{^1\text{H}\}$ NMR spectrum (0.05 M) and the cyanide region of the $^{13}\text{C}\{^1\text{H}\}$ NMR spectrum (0.1 M) of $\text{Ph}_3\text{PAu}^{13}\text{CN}$ (26% enriched) in CH_3OD : (A) 297 K; (B) 200 K ($^2J_{\text{PC}} = 126$ Hz).

constant of $^2J_{\text{PC}} = 126$ Hz, which is comparable to the value obtained for the $\text{Et}_3\text{PAu}^{13}\text{CN}$ complex ($^2J_{\text{PC}} = 122$ Hz in CH_3OD). The cyanide region of the ^{13}C spectrum at 297 K (Figure 5) has signals due to $\text{Ph}_3\text{PAu}^{13}\text{CN}$ (156.7 ppm, $^2J_{\text{PC}}$ not resolved) and $\text{Au}(\text{CN})_2^-$ (152.1 ppm). The slight difference between the observed chemical shifts for $\text{Au}(\text{CN})_2^-$ in the Et_3PAuCN system (151.4 ppm) and the Ph_3PAuCN system (152.1 ppm) is probably due to small changes in the temperature and/or concentration at which the spectra were accumulated. At 200 K, $\text{Ph}_3\text{PAu}^{13}\text{CN}$ appears at 156.1 ppm and $\text{Au}(\text{CN})_2^-$ is at 150.6 ppm. The coupling expected in the $\text{Ph}_3\text{PAu}^{13}\text{CN}$ complex is resolved ($^2J_{\text{PC}} = 126$ Hz) and is identical with that observed in the ^{31}P spectrum at 200 K. Thus, in solution, both Ph_3PAuCN and Et_3PAuCN disproportionate. The ligand-exchange processes occur at a faster rate for Ph_3PAuCN than for Et_3PAuCN since a lower temperature is required to resolve the resonances for the various species present.

Discussion

Cyano(triethylphosphine)gold(I) has been characterized in both the solid state and in solution. IR and Mössbauer spectroscopies demonstrate that in the solid state the complex exists as the neutral molecule and not as $[(\text{Et}_3\text{P})_2\text{Au}^+][\text{Au}(\text{CN})_2^-]$. The IR spectrum of solid Et_3PAuCN has only one cyanide frequency ($\nu_{\text{CN}} = 2138$ cm^{-1}). This value can be compared to 2141 cm^{-1} (IR) for $\text{KAu}(\text{CN})_2$ ¹⁷ and 2146 cm^{-1} for Ph_3PAuCN .⁹ The ^{197}Au Mössbauer spectrum (Figure 1) of Et_3PAuCN has IS (4.69 mm/s) and QS (9.56 mm/s) values that are typical of P-Au-C gold(I) complexes.¹⁸ These values can be compared to those reported for $\text{Au}(\text{CN})_2^-$ (4.36, 10.10 mm/s) and $\text{Au}(\text{PEt}_3)_2^+$ (5.40, 10.18 mm/s).¹⁸ The average isomer shift for these two complexes (4.88 mm/s) is, as might be expected, fairly close to that observed for Et_3PAuCN . However, the smaller value of QS for Et_3PAuCN as compared to the average QS of 10.14 mm/s is unusual if one considers the lower formal symmetry of the P-Au-C chromophore

(15) Mann, B. E.; Shaw, B. L.; Stainbank, R. E. *J. Chem. Soc., Chem. Commun.* **1972**, 151.

(16) Bosch, W.; Pregosin, P. S. *Helv. Chim. Acta* **1979**, 838.

(17) Jones, L. H. *J. Chem. Phys.* **1957**, 27, 468.

(18) Parish, R. V. *Gold Bull.* **1982**, 15, 51.

vs. the P-Au-P or C-Au-C chromophores. This anomaly may possibly be explained by using detailed comparisons of the local geometry and/or extended packing.

Unambiguous confirmation of the solid-state structure was achieved by determining the crystal structure (Figure 2, Table III). As expected for most two-coordinate gold(I) complexes, the molecule is essentially linear at the gold ($\angle\text{CAuP} = 176.6 (6)^\circ$) as well as at the cyanide ($\angle\text{NCAu} = 177 (2)^\circ$). The AuP distance of 228.8 (5) ppm is similar to $d(\text{AuP}) = 227.9$ pm in $\text{Ph}_3\text{PAuMe}^2$ and $d(\text{AuP}) = 225$ pm in $\text{Et}_3\text{PAuSATg}$ (SATg = tetraacetylthioglucose).¹⁹ The AuC distance of 197 (2) pm is comparable to $d(\text{AuCN}) = 201$ pm in $\text{AuCN}(\text{CNCH}_3)$ ²⁰ and to $d(\text{AuC}) = 202 (2)$ pm in $4\text{K}[\text{Au}(\text{CN})_2] \cdot \text{K}[\text{Au}(\text{CN})_2\text{I}_2] \cdot \text{H}_2\text{O}$.²¹ The large uncertainty in the bond length ($d(\text{AuC}) = 212 (14)$) for $\text{KAu}(\text{CN})_2$ precludes any meaningful comparison with that found here.²² The bond lengths reported for $\text{Ph}_3\text{PAuCN}^1$ ($d(\text{AuC}) = 185 (4)$ pm and $d(\text{CN}) = 125 (4)$ pm) are inconsistent with other values for gold cyanides and so are not used for comparison.²³

The NMR and solution IR studies demonstrated that in, for example, methanol solution Et_3PAuCN ($\delta_{\text{P}} = 35.1$ and $\delta_{\text{C}} = 160.4$), $(\text{Et}_3\text{P})_2\text{Au}^+$ ($\delta_{\text{P}} = 48.2$), and $\text{Au}(\text{CN})_2^-$ ($\delta_{\text{C}} = 151.4$) are in equilibrium with one another. This is, to our knowledge, the first clear evidence that, even in the absence of added ligands, neutral gold(I) complexes LAuX will disproportionate. Sadler has previously demonstrated in the reaction of glutathione and Et_3PAuCl that some disproportionation occurs, generating $(\text{Et}_3\text{P})_2\text{Au}^+$.²⁴ The equilibrium constant determined here is clearly solvent-dependent increasing with the polarity of the solvent. This is consistent with the formation of the ionic species $(\text{Et}_3\text{P})_2\text{Au}^+$ and $\text{Au}(\text{CN})_2^-$ according to eq 1.

- (19) Hill, D. T.; Sutton, B. M. *Cryst. Struct. Commun.* **1980**, *9*, 679.
 (20) Esperas, S. *Acta Chem. Scand., Ser. A* **1976**, *A30*, 527.
 (21) Bertinotti, C.; Bertinotti, A. *Acta Crystallogr., Sect. B: Struct. Crystallogr. Cryst. Chem.* **1972**, *B28*, 2635.
 (22) Rosenzweig, A.; Cromer, D. T. *Acta Crystallogr.* **1959**, *12*, 709.
 (23) We thank a reviewer for pointing out that the carbon atoms in metal cyanide complexes are sometimes mislocated by crystallography.
 (24) Razi, M. T.; Otiko, G.; Sadler, P. J. *ACS Symp. Ser.* **1983**, *209*, 371.

The analogous triphenylphosphine complex Ph_3PAuCN also crystallizes in the solid state as the neutral molecular species.¹ Previous IR studies of Ph_3PAuCN in CHCl_3 reported only a single cyanide stretch and concluded that Ph_3PAuCN is the only species present.⁹ Our ³¹P and ¹³C NMR results demonstrate that the complex disproportionates in solution and that the ligands exchange at a faster rate than for Et_3PAuCN . Since the ligand-scrambling reaction of Ph_3PAuCN is only observed at low temperature, there is the possibility that in other LAuX systems disproportionation may be similarly masked by rapid ligand exchange.

Labile ligand exchange is characteristic of gold(I), and it is therefore surprising that this type of disproportionation reaction has been previously overlooked or ignored. Such reactions may be very important in the biological milieu where the aqueous and therefore polar nature of intra- and intercellular compartments will facilitate similar disproportionation of gold drugs and their metabolites. It will be important to determine the effect of ligand basicity, bulk, and hydrophobicity on the extent and rate of these reactions.

Acknowledgment. A.L.H. and C.F.S. thank Smith Kline and French (SKF) for financial support and gifts of Et_3PAuCl . We acknowledge J. T. Guy and J. S. Rommel for assistance with the crystal structure, J. H. Zhang and M. J. Kwiecien for obtaining the Mössbauer spectrum, and F. Laib for obtaining the NMR spectra. A.L.H. also thanks the UMW graduate school for a graduate fellowship. W.M.R. acknowledges partial support of NSF DMR Solid State Chemistry Program Grant No. 8313710, USDOE Reactor Sharing Program Grant No. DE-FG02-80ER10770 to the MIT reactor, and SKF for funds for the purchase of the enriched Pt-source foil.

Registry No. Et_3PAuCN , 90981-41-2; Et_3PAuCl , 15529-90-5; Ph_3PAuCN , 24229-10-5; $(\text{Et}_3\text{P})_2\text{Au}^+$, 45154-29-8; $\text{Au}(\text{CN})_2^-$, 14950-87-9; $(\text{Ph}_3\text{P})_2\text{Au}^+$, 47807-21-6.

Supplementary Material Available: Table of final positional and thermal parameters (1 page); table of calculated and observed structure factors (6 pages). Ordering information is given on any current masthead page.

Contribution from the Laboratoire de Chimie Minérale, Université de Reims Champagne-Ardenne, F-51062 Reims, France

Dibromotris(*N,N'*-dimethylurea)manganese(II), a Pentacoordinated High-Spin Manganese Complex with Monodentate Ligands: Structure and Spectral Properties

Jacqueline Delaunay* and René P. Hugel

Received April 9, 1986

The high-spin complex dibromotris(*N,N'*-dimethylurea)manganese(II) crystallizes in the monoclinic system with $a = 13.211 (3)$ Å, $b = 8.670 (3)$ Å, $c = 16.593 (4)$ Å, $\beta = 106.23 (3)^\circ$, space group $C2/c$, and $Z = 4$. One of the characteristic features of this structure is the existence of neutral $\text{Mn}(\text{dmu})_3\text{Br}_2$ entities (dmu = *N,N'*-dimethylurea), showing a distorted bipyramidal geometry with monodentate ligands, the two bromine atoms lying in equatorial positions (point group C_2). The dmu ligands are bound by oxygen atoms, but two coordinative modes are observed: axial dmu ligands are classically bonded with a Mn-O-C angle of 129.5° , whereas equatorial dmu is unusually linearly bonded with an angle Mn-O-C of 180° . This goes with a significant shortening of the Mn-O equatorial bond length compared with the axial ones. The reflectance, Raman, and infrared spectra are interpreted on the basis of these results, as well as those of its isostructural analogous $\text{Mn}(\text{dmu})_3\text{Cl}_2$ complex. Force constants relative to MnO_3X_2 (X = Br, Cl) framework bonds have been calculated and are consistent with relative Mn-O bond length values. A $d \rightarrow \pi^*$ metal to ligand back-donation would explain the strengthening in the equatorial Mn-O bond, the *N,N'*-dimethylurea ligand herein exhibiting a π -acceptor role.

Introduction

High-spin manganese(II) complexes are characterized by the absence of ligand field stabilization energy, and this has two main consequences: (i) a lower stability of manganese(II) complexes compared with those of other metals of first transition series and (ii) the possibility to obtain various coordination geometries. Nevertheless, in regard to this last point, pentacoordinated complexes of manganese(II) are not common, and hereunder we report

such a case with monodentate ligands, for which a preliminary report appeared.¹

Despite the similarity of the two urea derivative ligands as *N,N'*-dimethylurea (L = dmu) and *N,N'*-diethylurea (L = deu), two different structures for the MnL_3Br_2 stoichiometry are ob-

(1) Delaunay, J.; Kappenstein, C.; Hugel, R. *J. Chem. Soc., Chem. Commun.* **1980**, 679.